CORONAL MASS EJECTIONS

CRISTIANA DUMITRACHE

Astronomical Institute of Romanian Academy
Str. Cutitul de Argint 5, 40557 Bucharest, Romania
crisd@aira.astro.ro

Abstract. The present work reviews the main theoretical aspects of the coronal mass ejections (CMEs) onset. We discuss the magnetic precursors, the basic models existing in the literature about the CMEs initiation. Numerical experiments of the CME in squalls are also outlined. The CMEs occurrence from the coronal streamers is also considered as an important source of the interplanetary disturbances.

Key words: coronal mass ejections, numerical simulations.

1. THE MAGNETIC PRECURSORS

The coronal mass ejections are spectacular manifestations of the erupting solar magnetism. They are the pieces of the Sun that travel in space and carry the solar activity out from the star. The solar activity has a fundamentally magnetic nature and so, the coronal mass ejections (CMEs) are magnetic phenomena. Coronal mass ejections represent one of the major events important for the solar activity action on the interplanetary space and consequently on our planet. The first CME detection belong to the Tousey's coronograph (1973) that was flown on OSO-7, who observed the coronal mass ejection occurred on 14 December 1971 with a velocity of 1000 km/s. Poland *et al.*(1973) also noted about Skylab observations the records of dynamic events with a lifetime ranging from minutes to days. These events produce significant coronal evolution and coronal features reorientations and have arch-like shape that expand with an approximate velocity of 500 km/s on a diameter over two solar radii. During time, many other such phenomena were observed in deferent wavelengths and scientist answered at many questions about their onset, propagation and effects. Numerical models have been performed and now we have an overall view on CMEs, but there are still many problems to be solved.

The CMEs are mainly produced by solar filaments that erupt or by energetic solar flares. In chapter 5 we have shown that recently there are some debates regarding the flares as source of CME. There are some authors that believe that CMEs onset produce flares. My opinion is that all cases are possible on the Sun. I analyzed observations where flares occurred in active regions destabilized the neighborhood filaments producing CMEs.

The CMEs are preceded by magnetic evolution during which magnetic flux emergence in the source regions induce helicity (van Driel-Gesztelyi *et al.*, 2002). The differential rotation acts on the emerging flux inducing helicity in the loops footpoints. When the magnetic flux exceeds a critical values, the magnetic structure blow up (see also chapter 4). Van Driel-Gesztelyi *et al.*(2002) found short-term magnetic precursors of the CME events as a combination of magnetic flux emergence, cancelation and fast shearing motions in active regions. They conclude that the magnetic topology that gives flares implies the existence of a magnetic null point low in the corona and a large-scale magnetic stress that lead to high helicity of the coronal loops. The CMEs coming from the filament eruptions imply the existence of a high level of helicity too, but a combination of flux emergence and flux cancelation that produce the stress.

An eruptive flare scenario was described by Aulanier *et al.*(2000): shearing motions in a delta-spot led the magnetic field lines to expand and reconnect. From these reconnections some field lines opened and released matter and energy, as flare and CME. This scenario is similar to the break-out model of Antiochos *et al.*(1999).

Totov and Demoulin (1999) discussed a model of a CME onset where a current sheet forms below a filament. If no reconnections are in region, the filament fall down and fast reconnections occur producing the filament eruption. This model implies reconnections with the material below the structure that erupt, while the break-out model implies reconnections with the material from above the erupting structure.

As result of numerical experiments, Liu *et al.*(2003) conclude that the initial magnetic configuration of the solar feature that give a CME is important and has influence on the CME kinematic properties. So, a normal polarity prominence gives high initial speed CMEs, while the inverse polarity prominence gives moderate speed CMEs.

2. THE BASIC CMES MODELS

The dynamo represents the motor of the solar activity and creates the magnetic field responsible for all the Sun manifestations, from the convective zone to the corona and out in the interplanetary space. The coronal features are based on the magnetic loops and arcades, that are the sites of birth of filaments, flares, coronal streamers and CMEs. The coronal loops stretch over the active regions and after complex processes they erupt to give flares or CMEs. The CMEs are pieces of plasma and magnetic field. After the eruption, when the magnetic field lines open, part of them reconnect back on the Sun and a similar process could continue many times, giving the so called CMEs ”en rafale”, or in squalls.

Modeling of these phenomena still constitutes a difficult challenge, with tasks

hard to accomplish. The MHD equations governing these phenomena are non-linear and for that the way of numerical simulations is the most common to follow. There were many attempts in the literatures, but some of them rest as landmarks of the topic. We remaind here Mikic *et al.*(1988), Biskamp and Welter (1989), Forbes (1990), Chen *et al.*(2001), Gibson and Low (1998), Antiochos *et al.*(1999), Wu *et al.*(2001), Amari *et al.*(2000), Odstrcil *et al.*(2002), Tokman and Bellan (2002), Linker *et al.*(2003), Roussev *et al.*(2003, 2004), Kusano *et al.*(2004).

The most difficult problem to solve for an unique model for initiation, development, propagation of a CME is linked to the different time scales and space grids involved in (from centimeters to few astronomical unities). This aspect is very suggestive summarized by (Forbes *et al.*, 2006) in figure 1.

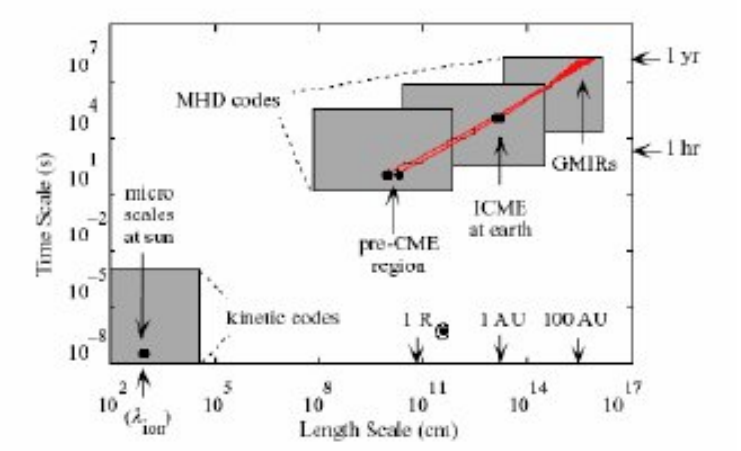

Fig. 1 – Time and length scales associated with CMEs as they propagate outwards through the heliosphere (Forbes *et al.*, 2006).

Considering that the origin of coronal mass ejection are prominences or flares or other type of structures, all these numeric codes start from a given initial magnetic field configuration and boundary conditions. Pursuit of its ejection from the place of the Sun to the interplanetary space require the running of multiple codes that works for different length scales. All these codes use the data output from one as input for the other.

The CME dynamics imply the consideration of a mechanism of initiation, but also the acceleration, the expansion, the drag force and distortion. A such complex code was developed by Odstrcil (2003) at George Mason University and NASA GSFC Space Weather Laboratory (`http://www.spaceweather.eu/ccmc-enlil`): it is ENLIL code. ENLIL is a time-dependent 3D MHD model of the heliosphere that

solves the equations for plasma mass, momentum and energy density, and magnetic field, using a Flux-Corrected-Transport (FCT) algorithm. Its inner radial boundary is located beyond the sonic point, typically at 21.5 or 30 solar radii. The real-time run uses Wang-Sheeley-Arge (WSA) for inner boundary conditions. The outer radial boundary can be adjusted to include planets or spacecraft of interest (eg 2 AU to include both Earth and Mars, 5 AU to include Ulysses, 10 AU to include Cassini). It covers 60 degrees north to 60 degrees south in latitude and 360 degrees in azimuth. A typical visualization of the results of this code looks like figure 2.

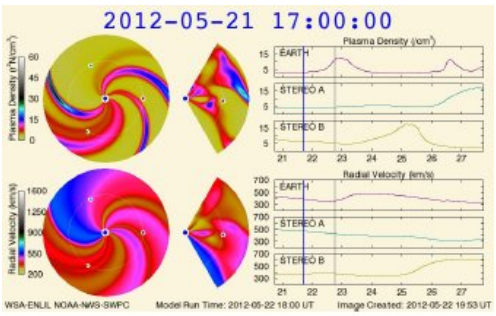

Fig. 2 – A typical result of a ENLIL code run.

An important aspect of evolution and CME propagation is that of determining the internal structure of interplanetary coronal mass ejection (ICME) in-situ magnetic field measurements. We will approach this topic in a later chapter of this book.

2.1. THE CMES INITIATION

Two classes of competing CME models could be differentiated: first by the magnetic topology criterium and, second, by the magnetic reconnection role in the CME process. After the first criterion, there are two types of initial magnetic configurations: the flux-rope and the sheared-arcade models. In the flux-rope models, it is assumed that a flux tube comprising a region in the corona of strong concentration of volumetric electric currents existing prior to the eruption. In the sheared-arcade models, it is assumed that a flux rope forms during the eruption. Considering the second aspect of the CMEs initiation, in the flux-rope models the magnetic reconnections are a consequence of the eruption, while in the other group the reconnections are the fundamental trigger of the ejection.

Most of models start from the presume that CMEs take their energy from the magnetic reconnections, like flares. The streamers that form in the solar corona as a consequence of the magnetic flux emergence lead to non-equilibrium states and push the field lines to magnetic reconnections to achieve a new equilibrium state. That is

the way of magnetic energy release and opening of the magnetic field line in corona. Part of the magnetic field and plasma are expelled in space as CME.

Currently there is no consensus on the mechanism that causes loss of balance – there are authors that consider the magnetic reconnections responsible for that, but there are other with a different opinion. Generally is accepted that a model should explain a mechanism responsible for the energy storage, but it seems that it is not always mandatory this. It is the case of the CME with small velocity with less than 150 km/s and a very small acceleration (Sirivastava *et al.*, 2000; Zhang *et al.*, 2004).

The storing energy models present an apparent paradox. They should explain how the magnetic energy decreases in the solar corona in spite of the fact that the CME sweeps away the magnetic field as it moves outward the Sun. Really, the magnetic energy increases and this is a paradox. Aly (1984, 1991) and Sturrock (1991) have showed that a magnetic field simply connected that open always has more energy than a free-force magnetic field. At first sight such a configuration is not possible, but the magnetic field may contain (a) knotted field lines and (b) field lines disconnected from the solar surface. Do not forget that, theoretically, a field line could goes to the infinite. The magnetic reconnections of the magnetic field lines are good to explain a lot of things.

We can distinguish three types of models for the CME initiation, in the literature:

- the flux ropes model and flow cancelation
- the field lines break out model
- the model with flow injection

The flux ropes model of the magnetic field lines could explain well the inverse polarity (IP) model of prominences given by Kuperus-Raadu (1974). The longitudinal magnetic field of the prominence is almost aligned to the filament channel (with a small angle between them, about 15^o), where the filament channel is on the opposite polarity inversion line at photospheric level. The IP prominence model implies the existence of a neutral point above the filament channel, point where the field lines cross and become on opposite sense to the photospheric magnetic field sense. This kind of magnetic configuration incorporates a great magnetic energy and a high degree of stress at its footpoints. A flux ropes bundle could appear in two distinct situations: it could emerge as it is from below the photosphere, or it could form as a consequence of the photospheric motions. This configuration could erupt after the magnetic field annihilation at the photospheric level. Sara Martin *et al.*(1985) define the magnetic field annihilation as the mutual disappearance of the field of opposite polarity to the neutral line. The elements of the flux flow and they annihilate each

other, or they dissipate in the solar atmosphere. This phenomenon was observed at filaments but also at the active regions in dissolution. This process seems to be present at small scale in the active regions, but also at the large scale, and it was modeled by Wang et.al. (1989). The magnetic field annihilation was associated to the solar flare (Livi *et al.*, 1989), but also to the coronal mass ejections (Lin *et al.*, 2004).

The magnetic field annihilation at the photospheric level is believed to be induced by the magnetic reconnections that trigger the CMEs by the loss of the equilibrium inside the flux tubes. A small current sheet forms in the reconnection zone and lift up in the solar atmosphere, by accomplishing successive stages of equilibrium until no one equilibrium could be possible and makes the structure to erupt. A great amount of energy is released on this occasion. The model of this scenario can be made only by numerical simulations.

The most popular accepted model of a coronal mass ejection initiation is that of the break out of the magnetic field lines (Antiochos *et al.*, 1999). In this model, the magnetic energy is stored in the field lines of a filament, lines that are high sheared and twisted until they are break out in a catastrophic way to release mass and energy.

The magnetic reconnections could produce in more types of magnetic topologies: in the break-out model they appear outside the filament channel, between the cvasi-potential magnetic filed of the prominence and the above surrounding coronal magnetic field. This case implies the existence of a multipolar magnetic topology that contain at least one neutral magnetic point as starting point of the reconnections. In the model that consider magnetic flux injection Chen (1989, 1996), the field lines erupt as a consequence of poloidal field injection. This model has been tested on a wide range of observations provided by SOHO spacecraft. Krall *et al.*(2001) showed that a distinct class of mass ejections obeys to this model and the solutions of it are in good agreement with the high-time profiles of CMEs observed by LASCO/SOHO.

Wu *et al.*(2000) distinct three CME initiation processes: streamer destabilization due to increase of currents via increase of axial fields, photospheric shears and plasma flow induced at the boundary region of a streamer and coronal hole.

Poedts *et al.*(2002) reviewed the numerical models for CME initialization and propagation and considered them as being in few classes:

(1) Directly driven models

(a) Thermal blast – characterized by a sudden release of thermal energy (Dryer, 1982; Wu, 1982) - CME associated with flares

(b) Dynamo models – real-time stressing of the magnetic field involves the rapid generation of coronal magnetic flux (Chen, 1989)

(2) Storage and release models – three classes in which a slow buildup of magnetic stress precedes the eruption

(a) Mass loading models – the field is loaded with mass (Low, 1999)

(b) Tether release models - the strain increase on a decreasing number of tethers (Forbes & Isenberg, 1991)

(c) Tether straining models – total stress increases (Antiochos *et al.*, 1999)

Forbes (2002) stated that a CME is triggered by the disappearance of a stable equilibrium as a result of the slow evolution of the photospheric magnetic field. This disappearance may be due to a loss of ideal-MHD equilibrium or stability such as occurs in the kink mode, or to a loss of resistive-MHD equilibrium as a result of magnetic reconnection.

3. OUR RESULTS FROM NUMERICAL SIMULATIONS

Our simulation is based on a prominence formation in a current sheet and its evolution. The current sheets naturally appear in the solar atmosphere. They are linked to the lines of magnetic polarity inversion line. They are places where prominences form and seldom their are at the base of a coronal streamer.

The MHD equations are solved with SHASTA method used by Alfven code, developed by Weber (1978). This code was described by Forbes & Priest (1982) and also by Dumitrache (1999).

$$\frac{\partial \rho}{\partial t} + \overrightarrow{\nabla}(\rho \cdot \overrightarrow{v}) = 0 \tag{1}$$

$$\rho[\frac{\partial \overrightarrow{v}}{\partial t} + (\overrightarrow{v} \cdot \overrightarrow{\nabla})\overrightarrow{v}] = -\overrightarrow{\nabla}(p) + (\overrightarrow{B} \cdot \overrightarrow{\nabla}) \cdot \overrightarrow{B} - \overrightarrow{\nabla} \cdot (\frac{B^2}{2}) + \rho \cdot \overrightarrow{g} \tag{2}$$

$$\frac{\partial \overrightarrow{B}}{\partial t} = \overrightarrow{\nabla} \times (\overrightarrow{v} \times \overrightarrow{B}) + \eta \overrightarrow{\nabla}^2 \cdot \overrightarrow{B} \tag{3}$$

$$\frac{\rho^\gamma}{\gamma - 1} \frac{d}{dt}(\frac{p}{\rho^\gamma}) = -\overrightarrow{\nabla}(k\overrightarrow{\nabla}T) - \rho^2 Q(T) + j^2/\sigma + h\rho \tag{4}$$

$$p = \rho T \tag{5}$$

The initial configuration is:

$$B_x = \begin{cases} \sin(\frac{\pi z}{2w}) & \text{for } |z| \le w \\ 1 & \text{for } |z| > w \end{cases} \qquad B_z = 0 \tag{6}$$

with $v_x = 0$, $v_z = 0$, where $w(= 0,25$ from the computation grid) is the thickness of the sheet , $\rho = 1$ and $p = \rho T$.

The imposed boundary conditions are:

– at top (x=1)

$$\frac{\partial B_z}{\partial x} = \frac{\partial B_z}{\partial x} = 0 \tag{7}$$

$$\frac{\partial B_z}{\partial x} = -\frac{\partial B_x}{\partial z} \tag{8}$$

– at right (z=1)

$$\frac{\partial B_x}{\partial z} = \frac{\partial B_z}{\partial z} = 0 \tag{9}$$

$$\frac{\partial B_z}{\partial z} = -\frac{\partial B_x}{\partial x} \tag{10}$$

– at left - the symmetry axis (z=0)

$$\frac{\partial B_x}{\partial z} = B_z = 0 \tag{11}$$

– at bottom (x=0)

$$\frac{\partial B_x}{\partial x} = \frac{\partial B_z}{\partial x} = 0 \tag{12}$$

4. CMES IN SQUALLS

Starting with a current sheet initial configuration and with $\beta = 0.5$ and $Rm = 10^3$, we performed this numerical experiment on 3 solar radii.

We obtain a prominences-like magnetic field configuration, after a cooling process in the sheet, at the Alfven time $t = 0.026$. The temperature in the sheet is about 5000 K. The figure 3 displays the magnetic field lines, the density and the velocity vector field. At this stage, downward motions are registered. The first CME starts at the Alfven time $t = 0.031$, very impulsively with a $v = 1245$ km/s. At $t = 0.036$ (see figure 3), the material is pushed to the lateral side of the current sheet and upward. Its velocity does dot exceed 420 km/s. The exhaustion of the matter is observed below the bubble, while the magnetic field picture displays plasma insulation. At $t = 0.040$ (figure 4) the loop is reformed, but plasma push strongly at the lateral side of the sheet. The legs of the previous ejecta are still visible on the figure. At $t = 0.042$, gravitational instabilities appear and the sheet is enlarged.

On the feet of the old prominences, the matter is upward moved: as result a new CME consisting from the leg's material, occurs. The velocity does not exceed

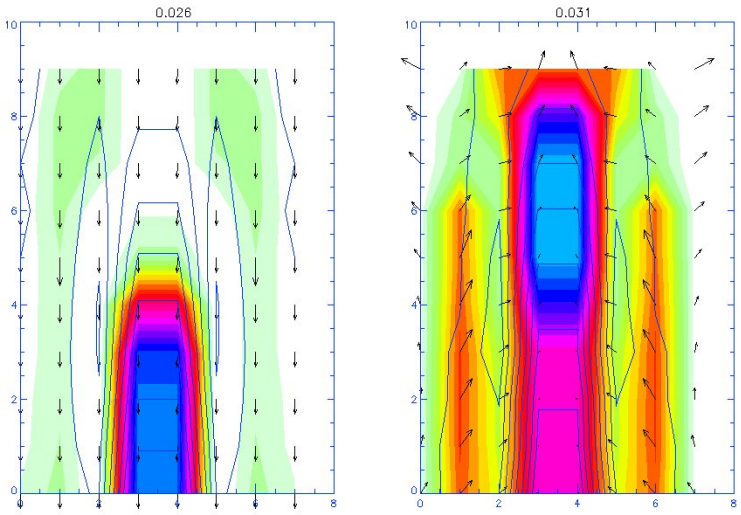

Fig. 3 – Alfven time $t = 0.026$ (left) and $t = 0.036$ (right).

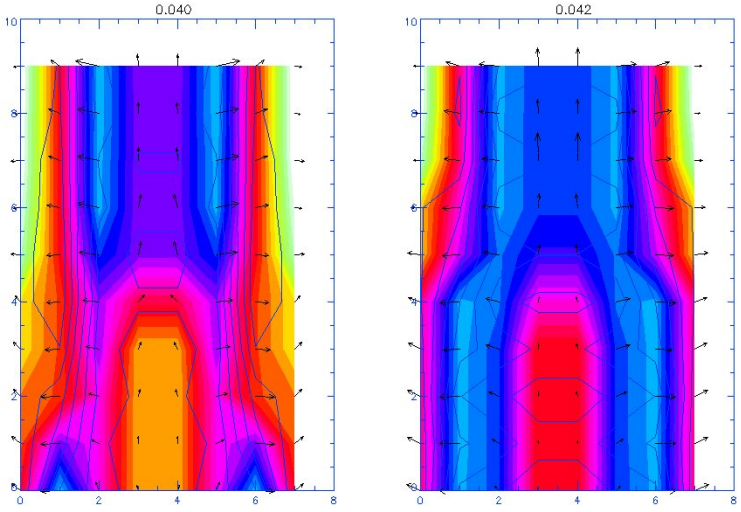

Fig. 4 – Alfven time $t = 0.040$ (left) and $t = 0.042$ (right).

620 km/s. From $t = 0.0453$ to $t = 0.053$ (figure 5) the legs are expelled in squalls. This could be considered as the second CME.

The process of the loop reforming replies at $t = 0.077$. During this time, after each CME, the temperature increased very much in the sheet and attains 10^6 K, so we have a hot coronal loop. We assist at a new magnetic reconnection, when the field lines open and a neutral O point forms below the bubble of plasma which elongated

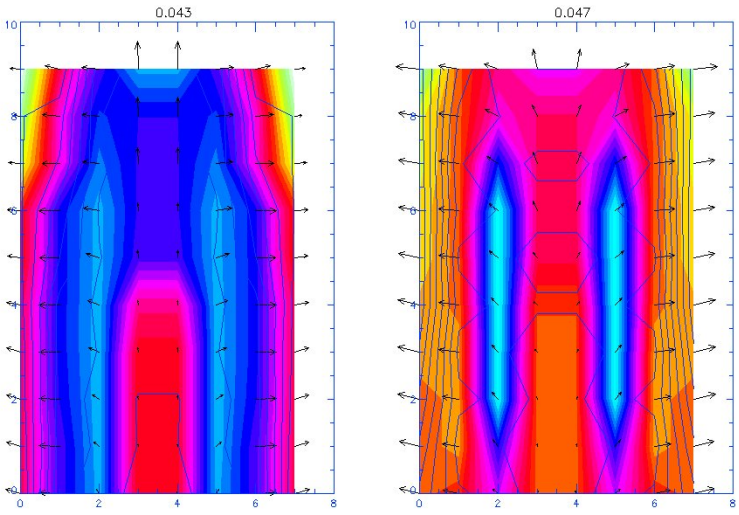

Fig. 5 – Alfven time $t = 0.043$ (left) and $t = 0.053$ (right).

to start in a new CME.

A new CME produce at $t = 0.085$ (figure 6), but with low velocity (160 km/s). The temperature of the ejected bubble reaches 2×10^6 K. After this CME, a coronal helmet streamer installed, starting with $t = 0.096$, with a temperature of 9×10^5 K at base and 1×10^6 K at top.

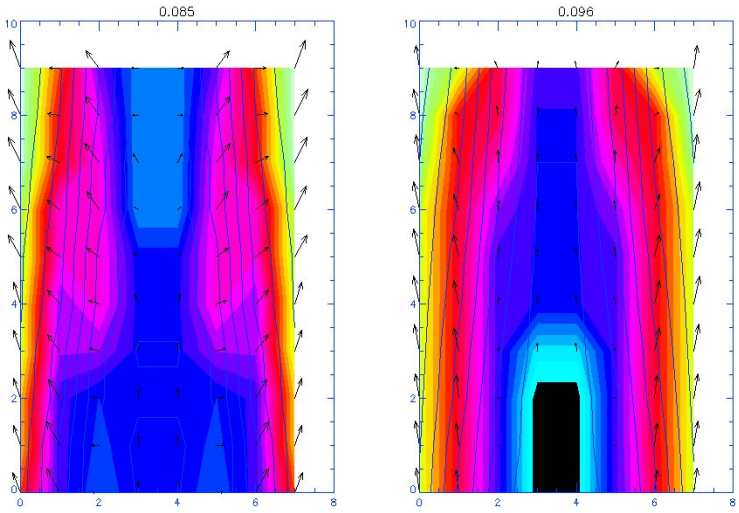

Fig. 6 – Alfven time $t = 0.085$ (left) and $t = 0.096$ (right).

The results translated in normal time show that the first CME produced after 1.7 hours, and the prominence formed in 1.5 hours. The second CME occurred after 2.08 hours. New mass collected in the sheet and a hot loop reformed. The lateral material pushing has determined gravitational instabilities and new CMEs produced, after 2.5 hours and 4.93 hours. After 6.3 hours, the structure evolved in a helmet streamer configuration (figure 6), which had its proper dynamics that our simulation follow till the streamer dissolution after 56 hours.

Our numerical experiment revealed a phenomenon similar to that observed also by SOHO on 27 March 2001, the so-called "cannibal coronal mass ejections". In our simulation, a prominence structure, formed in a current sheet, evolved in CME disruptions "en rafales". These transient phenomena in squalls are expression of the small-scale reconnections in the current sheet. The reconnections produced between two open field lines from both sides of a streamer current sheet and created a new closed field line (which becomes part of the helmet with a prominence at the base) and a disconnected field line, which moves outward. The CMEs are formed by plasma from the streamer that is swept up in the trough of the outward-moving field line.

5. THE CORONAL STREAMER ERUPTION

Another work (Dumitrache, 2000) refers to a helmet streamer formation, evolution and disruption, in case of mass emergence in the central part of the current sheet. The simulation was performed on ten solar radii. The results indicated that, during 20 days, the most dramatically changes were assigned to the streamer evolution: a lot of instabilities and a continuous grow up of the density. The velocity fields indicated upward motions inside the current sheet and downward movements on the lateral sides. Plasma insulated and stratified and the most dense region elongated starting with $t = 35.851$, so a helmet streamer configuration formed (figure 7).

At the end of the 20th day, at $t = 36.147$, the coronal structure get the aspect displayed in figure 7, when the mass injection was taken into account. The coronal helmet streamer destabilized and erupted in a CME at the Alfven time $t = 36.253$ (figure 8). At the beginning of the CME, the velocity reached almost 1800 km/s, but later the structure decelerated at 1400 km/s and even less.

What we have learned from this numerical experiment? Using a cartesian coordinates grid, we showed that a coronal streamer could form in a current sheet. The process is similar to the prominence formation and explain the apparition of the prominence-helmet streamer complexes in the solar atmosphere. When a flux emergence is taken into account, the structure destabilized and erupted in a CME, else the coronal streamer could have a gradually dissolution.

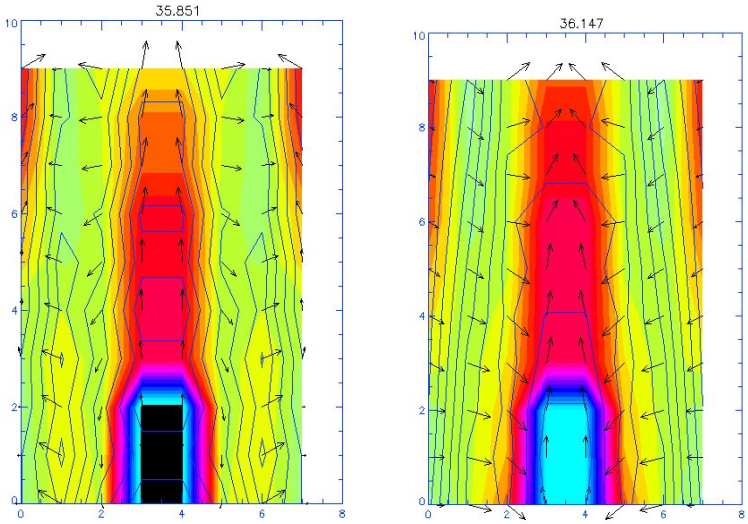

Fig. 7 – Alfven time $t = 35.851$ (left) and $t = 36.147$ (right)

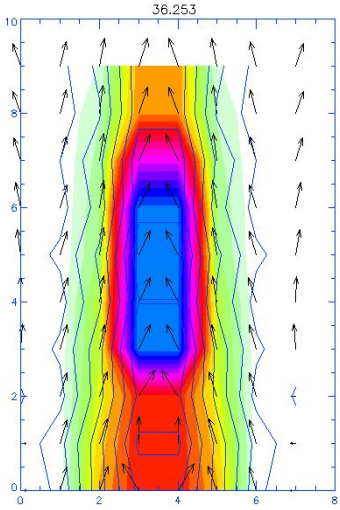

Fig. 8 – Alfven time $t = 36.253$

REFERENCES

Antiochos, S.K., Devore, C.R., Klimchuk, J.: 1999, *Astrophys. J.* **510**, 485.
Aulanier, G., DeLuca, L.L., Antiochos, S.K., McMullen, R.A., Golub, L.: 2000, *Astrophys. J.* **540**, 1126.
van Driel-Gesztelyi, L., Schmieder, B., Poedts, S.: 2002, *ESASP* **477**, 47.
Aschwanden, M. J.: 2004, *Physics of the Solar Corona. An Introduction*, Springer Verlag.
Aly, J. J.: 1984, *Astrophys. J.* **283**, 349.

Aly, J. J.: 1991, *Astrophys. J.* **375**, L61.
Amari, T., Luciani, J. F., Mikic, Z.,Linker, J. A.: 2000, *Astrophys. J.* **529**, L49.
Antiochos, S., DeVore, C., Klimchuk, J.: 1999, *Astrophys. J.* **510**, 485.
Berger, M. A: 1999, *Geophys. Monogr.* **111**, 1.
Berger, M. A., Field, G. B.: 1984, *J. Fluid Mech.* **147**, 133.
Biskamp, D., Welter, H.: 1989, *Solar Phys.* **120**, 49.
Chae J., Moon Y-J. , Park Y-D: 2004, *Solar Phys.* **223**, 39.
Chae, J., Jeong, H.: 2005, *JKAS* **38**, 295.
Chen, J.: 1989, *Astrophys. J.* **338**, 453.
Chen, J.: 1996, *J. Geophys. Res.* **101**, 27499.
Chen, P. F., Shibata, K., Yokoyama, T.: 2001, *Earth, Planets and Space* **53**, 611.
Demoulin, P., Berger, M. A.: 2003, *Solar Phys.* **215**, 203.
Dumitrache C.: 1999, *Romanian Astron. J.* **9**, 139.
Dumitrache, C.: 2000, *Physica Scripta* **62**, 510.
Dumitrache, C.: 2005,*PADEU* **15**, 45.
Fan Y.: 2004, *Living Rev. Solar Phys* **1**, 1.
Forbes, T.G., Priest, E.R.: 1982, *Solar Phys.* **81**, 303.
Forbes, T. G.: 1990, *J. Geophys. Res.* **95**, 11919.
Forbes, T.G., Isenberg, P.A.: 1991, *Astrophys. J.* 373, 294.
Forbes, T.G.: 2002, *Bull. of the American Astron. Soc.* **34**, 751.
Forbes, T. G., Linker, J. A., Chen,J., Cid, C., KoTa, J., Lee, M. A. , Mann, G., Mikic, Z., Potgieter, M. S., Schmidth, J. M., Siscoe,G. L., Vainio, R., Antiochos S. K., Riley,P.: 2006, *Space Sci. Rev.* **123**, 251.
Gibson, S. E., and Low, B. C.: 1998, *Astrophys. J.* **493**, 460.
Kuperus, M., Raadu, M. A.: 1974, *Astron. Astrophys.* **31**, 189.
Kusano, K., Maeshiro, T., Yokoyama, T., Sakurai, T.: 2004, *Astrophys. J.* **610**, 537.
Lee, J. K., Gary, G. A., Newman, T. S.: 2003, *Bull. of the American Astron. Soc.* **35**, 809.
Lin, J., Raymond, J. C., van Ballegooijen, A. A.: 2004, *Astrophys. J.* **602**, 422.
Linker, J. A., Mikic, Z., Lionello, R., Riley, P., Amari, T., Odstrcil, D.: 2003, *Phys. Plasmas* **10**, 1971.
Liu, W., Zhao, X. P., Wu, S. T., Scherrer, P.: 2003, in *Solar variability as an input to the Earth's environment. International Solar Cycle Studies Symposium*, (ed.) A. Wilson, *ESA SP* **535**, 459.
Livi, S. H. B., Martin, S. F., Wang, H., Guoxiang, A.: 1989, *Solar Phys.* **121**, 197.
Longcope, D. W., Welsch, B. T.: 2000, *Astrophys. J.* **545**, 1089.
Low, B.C.: 1999, *AIPC* **471**, 109.
Martin, S. F., Livi, S. H. B., Wang, J.: 1985, *Australian J. Phys.* **38**, 929.
Mikic, Z., Barnes, D., Schnack, D.: 1988, *Astrophys. J.* **328**, 830.
Odstrcil, D., Linker, J., Lionello, R., Mikic, Z., Riley, P., Pizzo, V., *et al.*: 2002, *J. Geophys. Res.* **107**, 1493.
Odstrcil, D.: 2003, *Adv. Space Res.* **32**, 497.
Pevtsov, A. A., Canfield, R. C., Metcalf, T. R.: 1994, *Astrophys. J.* **425**, L117.
Pevtsov, A. A., Canfield, R. C., Metcalf, T. R.: 1995, *Astrophys. J.* **440**, L109.
Pevtsov, A.A., Canfield, R.C., McClymont, A.N.: 1997, *Astrophys. J.* **481**, 973.
Pevtsov, A. A., Maleev, V. M., Longcope, D.W.: 2003, *Astrophys. J.* **593**, 1217.
Poedts, S., van der Holst, B., de Sterck, H., van Driel-Gesztelyi, L., Csik, A., Milesi, A., Deconinck, H.: 2002, *Proceedings of the Second Solar Cycle and Space Weather Euroconference* **477**, 263.
Poland, A.I., Gosling J.T., Hilder E.G., MacQueen, R.M., Munro, R.H., Ross, C.L.: 1973, *Bull. of the American Astron. Soc.* **5**, 419.
Roussev, I. I., Forbes, T. G., Gombosi, T., Sokolov, I. V., De Zeeuw, D., Birn, J.: 2003, *Astrophys. J.* **588**, L45.
Roussev, I. I., Sokolov, I.V., Forbes, T. G., Gombosi, T. I., Lee, M. A., Sakai, J. I.: 2004, *Astrophys. J.*

605, L73.
Seehafer N.: 1990, *Solar Phys.* **125**, 219.
Srivastava, N., Schwenn, R., Inhester, B., Martin, S. F., Hanaoka, Y.: 2000, *Astrophys. J.* **534**, 468.
Sturrock, P.: 1991, *Astrophys. J.* **380**, 655.
Titov, V.S., Demoulin, P.: 1999, *Astron. Astrophys.* **351**, 707.
Tokman, M., Bellan, P.: 2002, *Astrophys. J.* **567**, 1202.
Tousey, R.: 1973, *Bull. of the American Astron. Soc.* **5**, 419.
Wang, Y.-M., Nash, A. G., Sheeley, Jr. N. R.: 1989, *Science* **245**, 712.
Wang, J.: 1996, Solar Phys., **63**, 319.
Wu, S.T: 1982, *Space Sci. Rev.* **32**, 1150.
Wu, S. T., Andrews, M. D., Plunkett, S. P.: 2001, *Space Sci. Rev.* **95**, 191.
Zhang, J., Dere, K., Howard, R., Vourlidas, A.: 2004, *Astrophys. J.* **604**, 420.

Received on 4 November 2013